



**Acoustics'08
Paris**
June 29-July 4, 2008

www.acoustics08-paris.org

euronoise

Influence of Temperature Gradients on the Sound radiated from Flames

Rafael Piscoya and Martin Ochmann

Technische Fachhochschule Berlin, Univ. of Applied Sciences, Luxemburger Str. 10, 13353
Berlin, Germany
piscoya@tfh-berlin.de

The far field pressure of a turbulent flame can be determined using the standard boundary element method (BEM) if the sound pressure or its derivative is known at a closed surface (control surface) surrounding the flame, as long as the medium outside the control surface is homogeneous. If temperature gradients are present, the homogeneous Helmholtz equation is no more valid. In that case, the wave equation can be rewritten in form of an inhomogeneous Helmholtz equation with a source term that depends also on the unknown pressure. Using the “Dual Reciprocity BEM” the integral form of this wave equation can be solved involving only surface integrals, so that the sound field can still be computed from field values at the control surface. The cases under study consider a volume of hot gas with a temperature distribution that is prescribed or obtained from a CFD simulation. The influence of the temperature gradients on the sound field can be evaluated by comparison of characteristic quantities like sound power and radiation patterns, with and without temperature gradient.

1 Introduction

The prediction of the sound radiated from a turbulent flame is a very difficult task and cannot be handled efficiently with one method alone because of the disparity in time and length scales of the sound production and the sound propagation.

In previous works [1-3], a hybrid approach combining a Large Eddy Simulation (LES) with a Boundary Element Method (BEM) was implemented and used to compute the sound radiation of open turbulent flames. A key condition for the validity of this approach is to place the Kirchhoff surface in a homogeneous medium.

In many cases, it may be difficult to ensure that the Kirchhoff surface lies in a homogeneous medium. However, a large source region would demand a large computational domain leading to high computational effort. For these cases, the presence of an inhomogeneous medium has to be taken into account.

In the present work, the propagation of sound waves in an inhomogeneous medium is studied using an extension of the BEM, namely the Dual Reciprocity BEM (DRBEM).

2 Sound radiation of the flame

For the calculation of the radiated sound of a turbulent flame, it is assumed that at least one acoustic quantity, for example pressure p or particle velocity v_n is known at a closed surface S that encloses the flame (see Fig. 1).

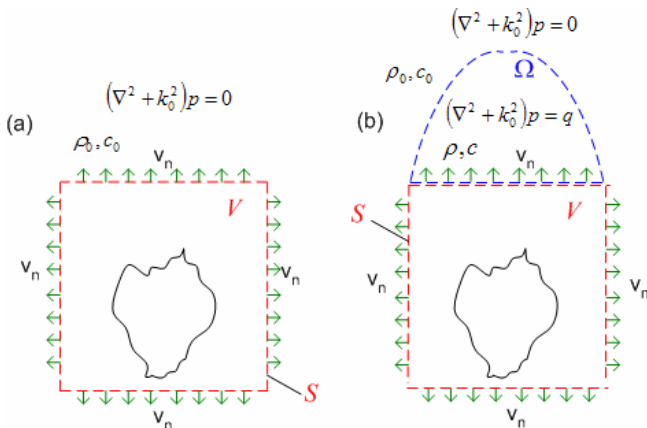


Fig.1 Models for an open flame; a) in a homogeneous medium and b) with a non homogeneous zone.

When the medium outside S is homogeneous (Fig. 1a), the sound field can be obtained by applying the standard BEM. Thus, the sound pressure at all points outside S is given by [4]

$$C(\bar{x})p(\bar{x}) = \int_S \left(p(\bar{y}) \frac{\partial g(\bar{x}, \bar{y})}{\partial n(\bar{y})} + j\omega \rho_0 v_n(\bar{y}) g(\bar{x}, \bar{y}) \right) dS(\bar{y}) \quad (1)$$

with the normal vector pointing to the outside,

$$G(\bar{x}, \bar{y}) = \frac{e^{-jk_0|\bar{x}-\bar{y}|}}{4\pi|\bar{x}-\bar{y}|} \quad \text{and} \quad C(\bar{x}) = \begin{cases} 1 & \text{outside } V \\ 0.5 & \bar{x} \in S \\ 0 & \bar{x} \in V \end{cases} \quad (2)$$

When the medium outside S is not homogeneous, Eq. (1) is no more valid. But a similar expression can be deduced if the inhomogeneities are written in form of a source distribution q , as it will be shown next.

Here, it is assumed that the inhomogeneous region occupies only a volume Ω and the rest of the fluid is homogeneous (see Fig. 1b). In this region, the density ρ and sound speed c may vary locally and differ from the ambient values ρ_0, c_0 .

To find the sound field outside S , the exterior space is divided in two regions and S is subdivided in two surfaces S_0 and S_1 as shown in Fig. 2. Region I is given by the volume Ω and limited by the surfaces S_2 and S_1 . Region II is the homogeneous zone outside $S_0 \cup S_2$.

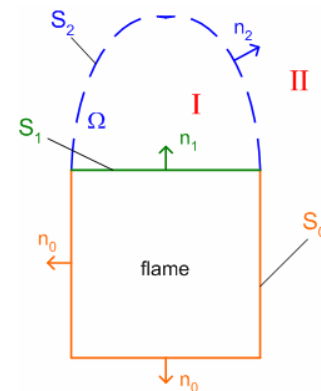


Fig. 2 Surfaces and domains for the sound field determination.

Two differential equations have to be solved

$$\begin{cases} (\nabla^2 + k_0^2)p_I = q & \text{Region I} \\ (\nabla^2 + k_0^2)p_{II} = 0 & \text{Region II} \end{cases} \quad (3)$$

with the boundary conditions

$$\begin{aligned} p_I &= p_{II} && \text{on } S_2 \\ \frac{1}{\rho} \frac{\partial p_I}{\partial n} &= \frac{1}{\rho_0} \frac{\partial p_{II}}{\partial n} && \text{on } S_2 \\ \frac{1}{\rho_0} \frac{\partial p_{II}}{\partial n} &= v_{nS} && \text{on } S_0 \cup S_1 \end{aligned} \quad , \quad (4)$$

where v_{nS} is the known particle velocity.

The integral equation for region II is given by Eq. (1) with the integration surface being $S_0 \cup S_2$. The integral equation for region I is given by [5]

$$\begin{aligned} C_I(\bar{x}) p_I(\bar{x}) &= - \int_{S_1 \cup S_2} \left(p(\bar{y}) \frac{\partial g(\bar{x}, \bar{y})}{\partial n(\bar{y})} + j\omega \rho v_n(\bar{y}) g(\bar{x}, \bar{y}) \right) dS(\bar{y}) \\ &\quad - \int_{\Omega} q(\bar{y}) g(\bar{x}, \bar{y}) dV(\bar{y}). \end{aligned} \quad (5)$$

Eq. (5) has an additional term with respect to Eq. (1), which corresponds to a volume integral over the source distribution q . To avoid the computation of the volume integral, the Dual Reciprocity method is applied to replace the volume integral with a series of surface integrals. This substitution is accomplished by expanding the source distribution in a set of functions f_j

$$q = \sum_j \alpha_j f_j \quad (6)$$

which are associated to another set of functions ψ_j through the inhomogeneous Helmholtz equation

$$(\nabla^2 + k^2) \psi_j = f_j \quad (7)$$

After applying the BE procedure to Eq. (7) and inserting the results together with Eq. (6) into Eq. (5), the final expression for the sound pressure in region I is

$$\begin{aligned} C_I(\bar{x}) p_I(\bar{x}) &= - \int_{S_1 \cup S_2} \left(p_I(\bar{y}) \frac{\partial g(\bar{x}, \bar{y})}{\partial n} + j\rho \omega v_{I,n}(\bar{y}) g(\bar{x}, \bar{y}) \right) dS + \\ &\quad \sum_j \alpha_j \left(C_I(\bar{x}) \psi_j(\bar{x}) + \int_{S_1 \cup S_2} \left(\psi_j(\bar{y}) \frac{\partial g(\bar{x}, \bar{y})}{\partial n} - \frac{\partial \psi_j(\bar{y})}{\partial n} g(\bar{x}, \bar{y}) \right) dS \right) \end{aligned} \quad (8)$$

$$\text{with} \quad C_I(\bar{x}) = \begin{cases} 1 & \bar{x} \in \Omega \\ 0.5 & \bar{x} \in S_1 \cup S_2 \\ 0 & \text{outside } \Omega \end{cases} .$$

Assuming that the source term q is known at some points of the volume, the coefficients α_j can be determined. Considering N points at the surface $S_1 \cup S_2$ and L points inside the volume Ω , and truncating the series (6) at $M=N+L$ terms, M coefficients α_j can be computed by solving the matrix equation:

$$\alpha = F^{-1} b \quad (9)$$

Here α and b are vectors with M components and F is a $M \times M$ matrix.

The discretization of Eq. (8) leads to the following matrix equation

$$C_I p_I + H p_I^s + j\rho \omega G v_m^s = \left(C_I \psi + H \psi^s - G \frac{\partial \psi^s}{\partial n} \right) \alpha \quad (10)$$

If the discretization is made at the same N points at the surface and L points inside the volume, and the boundary

conditions of Eq. (4) are taken into account, the pressure at the discretization points can be obtained.

3 Temperature gradient

In this work, the inhomogeneous region will be considered to have a local temperature distribution which is constant in time.

Since the sound speed and the density depend on the temperature, the wave equation becomes [6]

$$\frac{1}{c^2} \nabla \cdot (c^2 \nabla p_I) + k^2 p_I = 0 \quad (11)$$

By inserting the relation for perfect gases $c^2 = \gamma RT$ in Eq. (11), with γ and R constant, we get

$$\nabla^2 p_I + k^2 p_I + \frac{\nabla T \cdot \nabla p_I}{T} = 0 \quad (12)$$

The wave number $k = \omega/c$ depends also on the temperature. Adding and subtracting the term $k_0^2 p_I$ and rearranging the terms we obtain:

$$\nabla^2 p_I + k_0^2 p_I = q \quad , \quad q = (k_0^2 - k^2) p_I - \frac{\nabla T \cdot \nabla p_I}{T} \quad (13)$$

Eq. (13) shows that the source term q contains the derivatives of the unknown variable p_I . In this case, p_I has to be expanded in a series of functions d_j in a similar way as was performed for q , so that its derivatives can be defined in terms of the derivatives of the known functions d_j :

$$p_I(\bar{x}) = \sum_j \beta_j d_j(\bar{x}) \rightarrow \nabla p_I(\bar{x}) = \sum_j \beta_j \nabla d_j(\bar{x}) \quad (14)$$

4 Numerical example

The procedure described in section 3 for an open flame can be very well applied to study the sound radiation of a semi closed flame. It is assumed that the flame is placed inside a cylindrical combustion chamber that has one open end. The sound waves coming out through the opening are characterized by the velocity at the opening. On the other hand, the sound waves in the chamber may induce vibrations of the chamber walls that radiate sound to the outside and contribute to the total emitted sound.

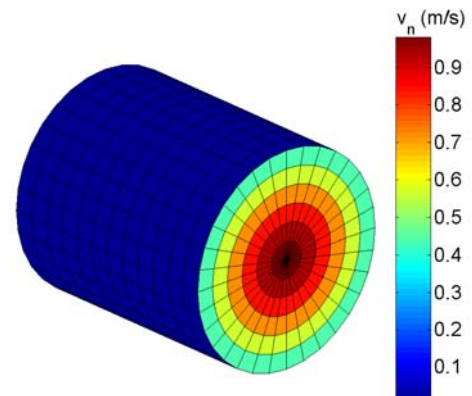


Fig. 3 Velocity distribution at the cylindrical surface.

In our example, the chamber walls are assumed to be rigid, so that no vibrations arise. Thus, the normal velocity at the walls is zero. At the open end, a radial velocity distribution is considered (see Fig. 3). Outside the combustion chamber, next to the open end, a temperature distribution

$$T(x,y,z) = T_m \exp\left(-\mu \frac{A(y^2 + z^2)}{x_0 - x}\right) \quad (15)$$

in a region of length L_T is prescribed. In Eq. (15), A and x_0 are constants, $\mu = \ln(T_m/T_a)$ and T_m and T_a are the maximum and ambient temperature respectively.

The effect of the temperature distribution was studied by varying T_m and L_T . Three different values of L_T were considered: 0.7R, 1.4R and 2R. The maximum temperatures investigated were 50°C, 100°C, 200°C, 300°C, 400°C and 500°C. In Fig. 4, the temperature distribution is shown for two values of T_m .

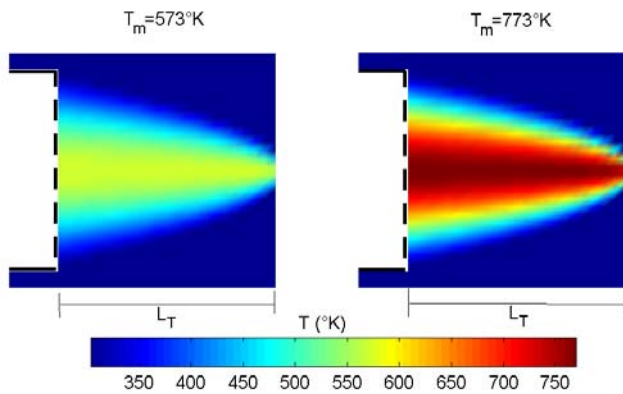


Fig. 4 Temperature distribution.

The variation of the sound speed and the density with the temperature was obtained by using the relations:

$$c = 20.05 \sqrt{T(^{\circ}K)} \quad , \quad \rho = 360.77819 T(^{\circ}K)^{-1.00336} .$$

For the numerical computation of the sound field, the combustion chamber was modeled with a cylinder of length 0.5 m and a radius of 0.22 m. The cylinder had 768 elements. The inhomogeneous region was limited by a paraboloid of revolution. For $L_T=0.7R$ the surface had 224 elements, for $L_T=4R$, the surface had 800 elements. The number of interior points for the approximation of the source term was 200 for the shorter region and 500 for the larger one. The surface models and interior points are shown in Fig. 5.

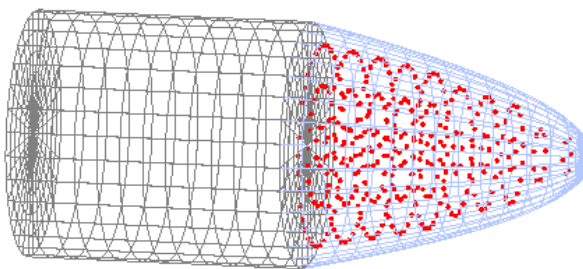


Fig. 5 Surface models and interior points ($L_T=2R$).

The approximation functions f_j and associated functions ψ_j that were used are given by

$$f_j = 1 + r_j \quad ,$$

$$\psi_j = \frac{1 + r_j}{k_0^2} - \frac{2(1 - \cos(k_0 r_j))}{k_0^4 r_j^2} \quad (16)$$

$$d_j = 1 + r_j^3$$

where $r_j = |\vec{x} - \vec{y}_j|$ is the distance from the field point \vec{x} to the surface or interior point \vec{y}_j .

In a previous work [7], these functions were tested using a “spherical flame” with different source distributions. For some specific type of sources, the problem has an analytical solution. The numerical solutions showed very good agreement with the analytical ones.

The results of the calculations are presented in figures 6 – 9. In first place, we analyze the effect of the temperature distribution on the sound power. The sound power increases at low frequencies and reaches some approximately constant value at high frequencies. This constant value decreases uniformly with increasing T_m . This effect could be explained considering that more energy is reflected back into the hot region if the temperature is higher.

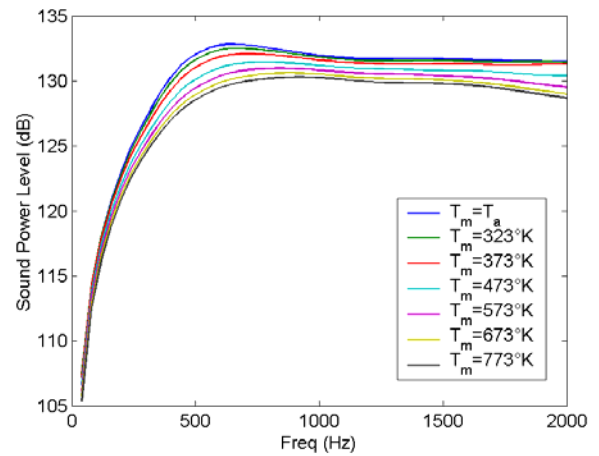


Fig. 6 Dependence of the sound power with the maximum temperature.

The length of the hot region appears to have less influence on the sound power than the temperature itself. In Fig. 7, the sound power for $T_m=773^{\circ}K$ and three different values of L_T is shown. The differences can be seen principally at high frequencies and they are small.

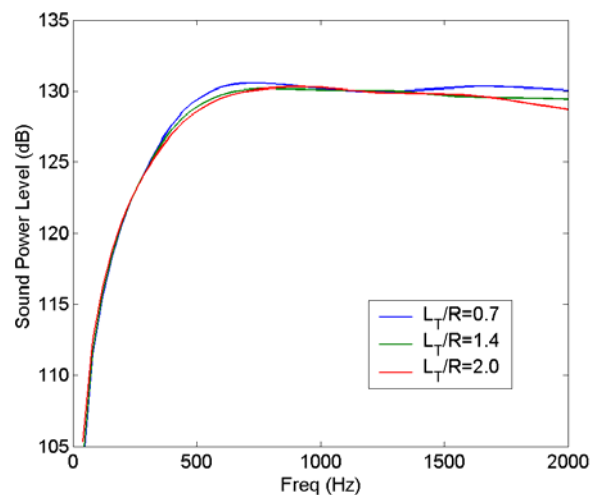


Fig. 7 Dependence of the sound power with the length of the hot region.

The influence of the temperature on the radiation patterns is illustrated in Fig. 8. The polar plots show the sound pressure level normalized to the maximum value at a spherical surface with a radius of 100 m. It can be observed that the higher the temperature, the broader the radiation patterns become. This effect is caused by the refraction of the sound waves in the hot region due to the variable sound speed.

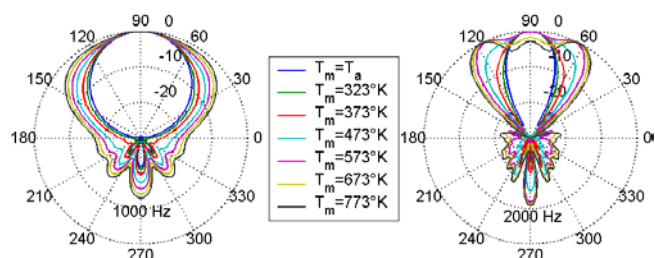


Fig. 8 Dependence of the radiation pattern with the maximum temperature.

The radiation patterns appear to be more sensitive to the length of the hot region than the sound power. The larger the hot region, the broader the radiation pattern becomes. This effect is shown in Fig. 9. The polar plots are calculated for two frequencies for $T_m=773^\circ\text{K}$.

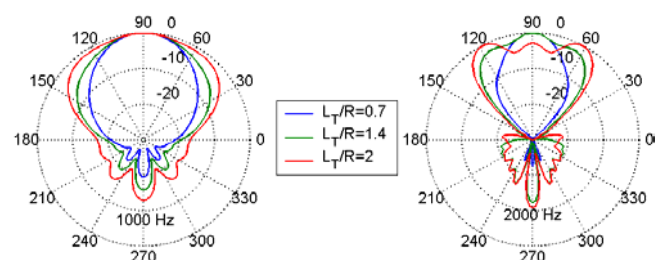


Fig. 9 Dependence of the radiation pattern with the length of the hot region.

5 Conclusion

The sound propagation in an inhomogeneous medium can be treated by using the Dual Reciprocity BEM if the differential equation can be written as an inhomogeneous Helmholtz equation with source terms appearing at the right hand side. This approach was applied to study the propagation of sound waves coming from a combustion chamber in the presence of a hot region with temperature gradient at the chamber exit. The sound waves are refracted away from the axis producing broader radiation patterns and partially reflected leading to a decrease of the radiated power.

Acknowledgments

This work is integrated in the research unit "Combustion Noise Initiative", supported by the German Research Foundation (DFG) [8].

References

- [1] H. Brick, R. Piscoya, M. Ochmann, P. Költzsch, "Prediction of the Sound Radiated from Open Flames by Coupling a Large Eddy Simulation and a Kirchhoff-Method", *Proc. Forum Acusticum*, Budapest (2005).
- [2] R. Piscoya, H. Brick, M. Ochmann, P. Költzsch, "Application of equivalent sources to the determination of the sound radiation from flames", *Proc. 13th International Congress on Sound and Vibration*, Vienna (2006).
- [3] R. Piscoya, H. Brick, M. Ochmann, P. Költzsch, "Equivalent Source Method and Boundary Element Method for calculating combustion noise", *Acta Acustica united with Acustica*, accepted for publication, (2008).
- [4] M. Ochmann, "Analytical und Numerical Methods in Acoustics" in Mechel. F.P.: *Formulas of Acoustics*, 930-1026, Springer, (2002).
- [5] L. C. Wrobel, *The boundary element method - Vol. 1: Applications in thermo-fluids and acoustics*, Wiley, (2002).
- [6] S. W. Rienstra, A. Hirschberg, *An Introduction to Acoustics*, Eindhoven University of Technology, (2004).
- [7] R. Piscoya, M. Ochmann, "Sound propagation in a region of hot gas using the DRBEM", *Proceedings 14th International Congress on Sound and Vibration (ICSV14)*, Cairns, Australia (2007).
- [8] Combustion Noise Initiative, URL: <http://www.combustion-noise.de>